Noname manuscript No.
(will be inserted by the editor)

Sequential sphere packing by trilateration equations

To H. D. · Galindo-Torres S. A. · Scheuermann A.

Received: date / Accepted: date

Abstract Specimen generation by packing of particles is the initial step in most numerical simulations for discrete media. In many cases, especially for virtual soil compaction, filtration, or penetration tests, this preparation work is essential for the success of the tests because the discrete particles are not able to be redistributed during the simulation. This paper presents a novel sphere sequential packing method for specimen generation using the trilateration method and its relevant equations. The method is developed on an assumption that all particles must be in contact with at least three neighboring particles to be kept in balance. This semi-analytical method has three advantages: quick generation speed, adjustable porosity, and good control over the spatial distribution of particles at a local scale. This paper is a study on two typical spatial distributions: (1) layer-wise, where particles with similar sizes have priority of being placed next to each other; and (2) discrete, where small particles are located preferentially in between large particles.

Keywords Sphere · sequential packing · trilateration equations · semi-analytical · spatial distribution · porosity · discrete element · general shape

*Corresponding author: To Huu Duc, School of Civil Engineering, The University of Queensland
AEB, Staff House Road, Brisbane, QLD 4072, Australia
Tel.: +61 4 2288 2226
E-mail: h.to@uq.edu.au

Sergio Andres Galindo-Torres, Geotechnical Engineering Centre, School of Civil Engineering, Research Group on Complex Processes in Geo-Systems, The University of Queensland · Alexander Scheuermann, Geotechnical Engineering Centre, School of Civil Engineering, Research Group on Complex Processes in Geo-Systems, The University of Queensland

1 Introduction

Soil is a discrete porous medium, which comprises individual soil particles. Therefore, the arrangement of particles may have a significant influence on the hydraulic and mechanic features of the soil as a bulk. For instance, with the same multi-gap-graded *Particle Size Distribution* (PSD), but different spatial arrangement of particles, a soil specimen might form a multi-layer filter or an erodible structure.

In general, most computational simulations for discrete media start with generating specimens acquired from a particle packing process. This preparation work may play a decisive role in the establishment of soil features. In addition, these features might be unchangeable because particles cannot be moved or reoriented easily later on.

It is well acknowledged that the spherical shape is currently one of the most popular particle shapes employed in discrete soil simulations because of its simplicity. Conventionally, there are two common approaches to pack non-uniform spherical particles: instant and sequential. In the first approach, particles are generated as a bulk within a container. In order to create a granular structure, particles are subsequently forced to settle by either compacting or dropping [1], or resizing and rearranging [2,3]. Usually the Discrete Element Method (DEM) is employed for this task, which can be very time consuming. In the second approach, particles are placed sequentially into a given volume by dropping and rolling [4,5,6] or looping and resizing [7,8].

A serious challenge for both approaches is the accomplishment of a given porosity without changing a predefined PSD. If particles with the predefined PSD are generated first, that is, as a bulk, they might not completely fill the estimated volume to reach the de-

sired porosity because of their inappropriate packing. A subsequent compaction of the specimen is possible only to a limited extent because spheres, having the same dimension by all directions, cannot be compacted by reorientation. Contrariwise, if the desired porosity is approached first, it is a huge challenge to resize and rearrange particles in a way to achieve a stable granular structure using the predefined PSD, while the desired porosity is preserved.

This paper represents a novel sequential sphere packing method, which employs trilateration and relevant equations to pack spheres with a predefined PSD and porosity. Although the simulation with particles of general shapes has been achieved recently by some researchers [9,10], including the authors [11,12], spheres as particles are used in the presented method because of theirs simplicity and applicability to sandy soils. Positive features of the presented method are time efficiency and good control over the local particle distribution.

In terms of position control, the method allows the arrangement of particles in two different ways: layer-wise and discrete. The layer-wise arrangement gives priority to particles with similar radii to be placed next to each other in order to achieve a local narrow-graded PSD. This arrangement has a very practical meaning in the sense of soil structures created by segregation, for example, when soils are dumped from trucks on construction sites. For the discrete arrangement, fine particles are preferably placed in the voids among coarser particles. Therefore, the specimen is more homogeneous.

2 Methods

2.1 Main algorithms

The basic idea of the new packing method originates from simple considerations of the static stability of any kind of element to be added to an existing structure. Therefore, the new method assumes that a sphere should have at least three contacts with its neighbours to find a statically stable position, or four contacts to be kept firmly in the structure enabling transfer of loads (Figure 1).

The main algorithm consists of several calculation steps (Figure 2):

- Firstly, data is imported from some input text files (step 1), which contain soil PSD, porosity, volume, and other packing parameters, such as maximum length of size intervals.
- The PSD is divided into *ni* small intervals, each of which is represented by a mass fraction and a characteristic mean size. This fact makes calculated PSD multi-gap-graded at some level (Figure 3). However, when the number of size intervals increases, this effect diminishes. In addition, the sieving process provide only for particles up to the maximum diameters passing through, but no information about the size distribution in between sieving sizes. Hence, it is safe to say that the calculated PSD is one possible PSD for the given data.
- Based on a given volume to be filled (e.g. of a container) and a predefined porosity, a list of particles is generated complying with the predefined PSD.
- An initial face is built from the central coordinates of the first three mutually tangent particles (step 3). To avoid the lack of space for subsequent coarse particles (Figure 3), the first particle should be the biggest, and needs to be placed at the centre of the soil volume. Actually, this does not influence the reality of packing because if that particle is not located at the centre, the volume can be shifted to obtain that condition.
- A new particle is selected from the list (step 4) to be placed by trilateration equations (Equation 1). Then, the arrangement is checked to estimate whether there is an overlap between the new particle and existing ones or the boundary of the given volume (step 5).
- In case an overlap exists, the new particle can be moved or resized (step 6) to avoid the overlapping particle (Figure 4). This seeking position process is interrupted when the new position of the added particle is extremely poor, that is, too far from the face or beyond the boundary of the soil specimen.
- If the particle is too far away, the overlapping particle might be used as a substitute to build up a new tetrahedron on the face (step 7).
- When the new particle does not overlap with all existing ones, a tetrahedron will be built from the central coordinates of these four particles (step 7). This tetrahedron possesses three new 'open' faces, to which new particles can be added, and one existing face, which is defined in step 8 as 'closed' (no new particle can be added to that face). Similarly,

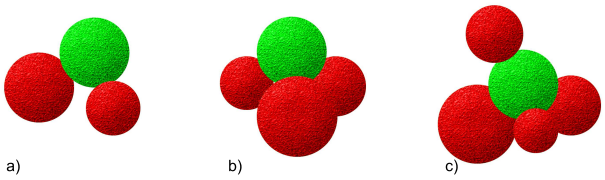

Fig. 1 Contacts of a spherical particle with surrounding ones: a) Non stable contact; b) stable contact; c) firm contact.

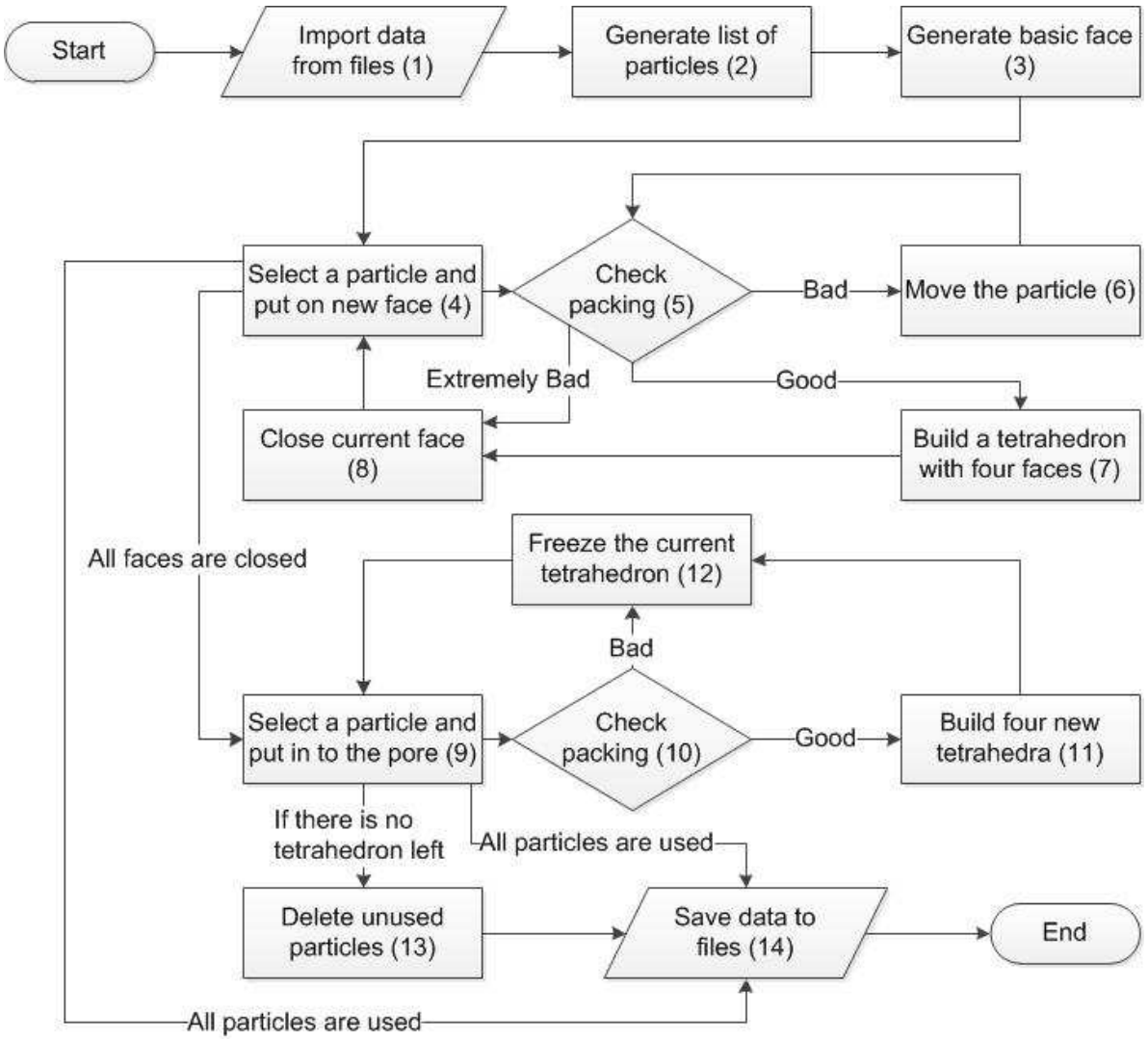

Fig. 2 Main packing algorithm. The packing is facilitated by a comprehensive library of function in C++, which can be downloaded from an authors' website [13]. Besides, this library is also attached to a broader open source domain dealing with a range of numerical methods [14].

the new added particle also will be marked as a 'used' particle.
- The process (step 4 - 8) is repeated with new particles and a new faces until either all particles are used or no more open faces exist.
- In the case where all faces are closed, but unused particles still exist, an unused particle is selected from the list and placed into a pore with sufficient size of tetrahedron by Equation 3 (step 9). Overlapping of the new arrangement is checked and corrected if necessary(step 10). Because of the discrepancy between radii of pores and particles, the new particle might not have contacts with other particles. A stable network can be approached after stabilization, which will be described below.
- If the new particle is placed successfully, four new tetrahedra are created (step 11) by the central coordinates of the new particle and the four faces of the existing tetrahedron, which is defined as 'frozen' in step 12. This filled tetrahedron might be eliminated to avoid the confusion with four new tetrahedra.
- The process (step 9 - 12) is repeated with other tetrahedra until all tetrahedra are frozen or all particles are used.
- All unused particles are reported and eliminated (step 13) before data export (step 14).

Obviously, the algorithm does not always successfully place all generated particles in a predefined container to achieve the given PSD, especially when the porosity is too low. This pathological case can be identi-

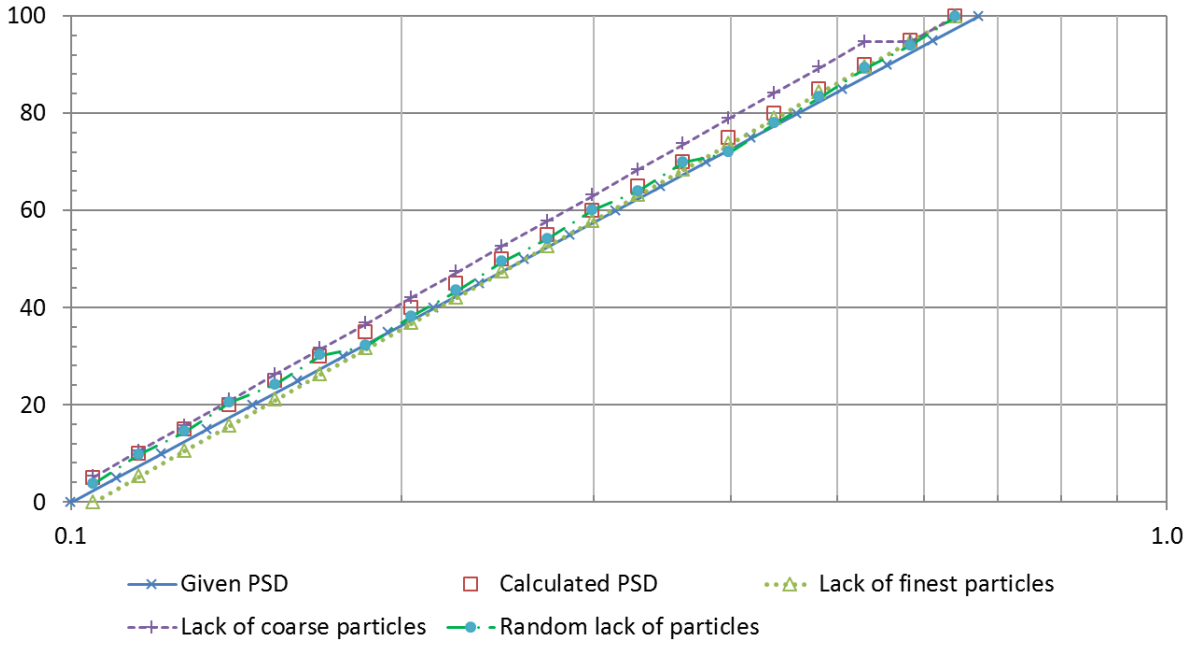

Fig. 3 Expected and approached Particle Size Distribution (PSD). A typical, given logarithmic distribution is divided in to several intervals for particle generation. If the number of intervals, ni, is large enough, the lack of particles in an interval might not seriously influence on the general PSD.

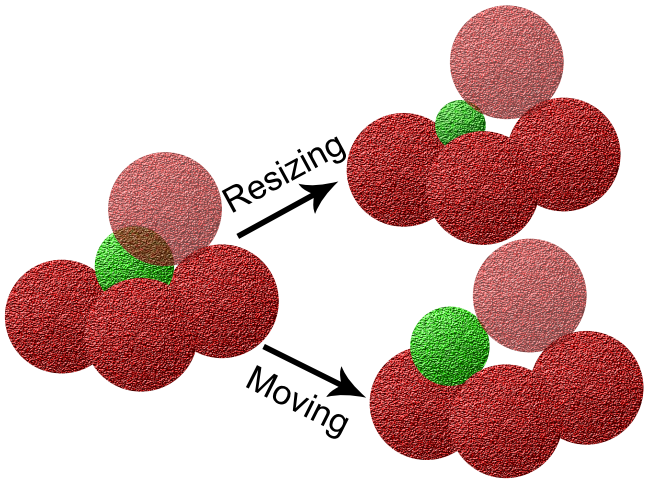

Fig. 4 Adjustment of particles added to a built face of an existing arrangement (step 5). If an overlap with another particle (light red) exists, the new particle (green) can be moved to another position inside the predefined volume, or the added particle can be resized by an exchange with a smaller particle as long as the size is not forced to be large (e.g. for layer-wise arrangement).

fied easily by the report of an unused particle. When the layer-wise arrangement is employed, the unused particles often have small sizes. Meanwhile, the distribution of unused particles by discrete arrangement is more random (Figure 3).

Contrariwise, the given volume may not be fully filled with particles if the porosity is too high. This problem can be identified by visualisation or by the stabilization simulation which will be described later.

Nevertheless, the new method can alter successfully the porosity of specimens in a range by good control on particle distribution, which is facilitated by trilateration and relevant equations.

2.2 Trilateration equations

As mentioned above, trilateration and its relevant equations are adopted to add particles to the specimen during the packing process (step 4, 6, and 9). These equations were often employed in the initial Global Positioning System technology to estimate the coordinates of an object when the distances from it to satellites were known [15].

Before the application of trilateration equations, particle coordinates are converted from the global coordinate system to the local one (Figure 5) in order to ease the solution of the equations and to avoid the 'division by zero' error, what can happen when two particles are aligned with an axis. The trilateration equations in the local coordinate system transform to:

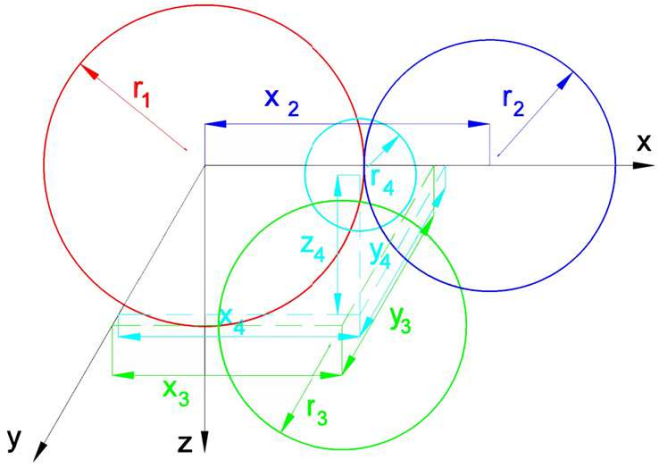

Fig. 5 Local coordinate system for an arrangement of four particles. Particles 1(red), 2 (blue), and 3 (green) form the face and particle 4 (cyan) is added.

$$\begin{aligned} x_4^2 + y_4^2 + z_4^2 &= (R_4 + R_1)^2 \\ (x_4 - x_2)^2 + y_4^2 + z_4^2 &= (R_4 + R_2)^2 \\ (x_4 - x_3)^2 + (y_4 - y_3)^2 + z_4^2 &= (R_4 + R_3)^2 \end{aligned} \quad (1)$$

Where: x_i, y_i, z_i, and R_i - central coordinates and radii of particles i.

When the new particle is smaller than the constriction between existing particles, it cannot touch all three existing particles. In this case, Equation 1 has no root. The new particle can be placed next to two particles on the face, or at the centre of the constriction formed by existing particles on the face (Figure 6):

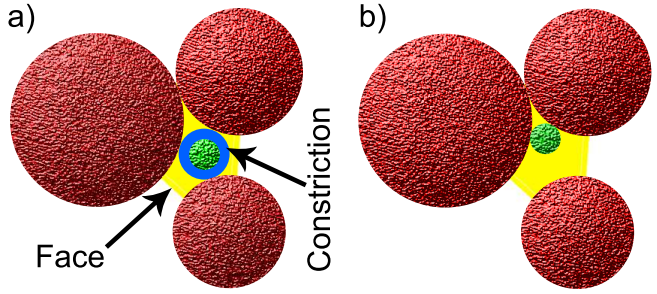

Fig. 6 Adjustment for particles smaller than constriction size. The added particle can be placed: a) at the centre of the constriction, or b) mutually tangent with existing particles forming the face.

$$\begin{aligned} x_c^2 + y_c^2 &= (R_c + R_1)^2 \\ (x_c - x_2)^2 + y_c^2 &= (R_c + R_2)^2 \\ (x_c - x_3)^2 + (y_c - y_3)^2 &= (R_c + R_3)^2 \end{aligned} \quad (2)$$

Where: x_c, y_c, z_c, and R_c - central coordinates and radius of the constriction.

Geometrically, the constriction is the narrowest place along the path connecting pores. Note should be taken here of the constriction size distribution which also is a very important feature of soils for internal instability assessment [16] and some other seepage flow simulations.

Regarding the second loop, a particle is placed into a pore (step 9) by solving the following relevant equations:

$$\begin{aligned} x_p^2 + y_p^2 + z_p^2 &= (R_p + R_1)^2 \\ (x_p - x_2)^2 + y_p^2 + z_p^2 &= (R_p + R_2)^2 \\ (x_p - x_3)^2 + (y_p - y_3)^2 + z_p^2 &= (R_p + R_3)^2 \\ (x_p - x_4)^2 + (y_p - y_4)^2 + (z_p - z_4)^2 &= (R_p + R_4)^2 \end{aligned} \quad (3)$$

Where: x_p, y_p, z_p, and R_p - central coordinates and radius of the pore.

Obviously, these equations in the local coordinate system can be solved much more easily than the original trilateration equations in the global coordinate system. All equations become one quadratic equation because unknown coordinates can be estimated by a function of radius. Only real positive roots are considered. There are already some mathematical solutions for equation 3 which can be used as alternative methods [17,18]. The pore and constriction sizes limited by particles and a spherical boundary can be calculated, if needed, by assuming the boundaries is a virtual particle with negative radius (Figure 7). A similar calculation with polyhedral and cylindrical boundary is more complicated because of the identification of limiting boundary faces.

When the particles are mutually tangent to each other, Equations 2 and 3 can be replaced by the solution of the Descartes theorem or the Soddy Gosset theorem [19]. Then, the radius of the constriction and/or pore can be calculated from the radii of existing particles:

$$\left(\sum_{i=1}^{d+2} \frac{1}{R_i}\right)^2 = d \sum_{i=1}^{d+2} \frac{1}{R_i^2} \quad (4)$$

Where: d - the dimension of Euclidean space, $d = 2$ (for constrictions) or 3 (for pores).

In many cases the added particle does not perfectly tangent the existing particles, which results in moving or resizing the particle (step 6). As a consequence there might be particles within the overall package with less than three contacts. If the package is used for further simulations which require a firm particle structure, for example, oedometer tests, the overall arrangement of particles must be stabilised.

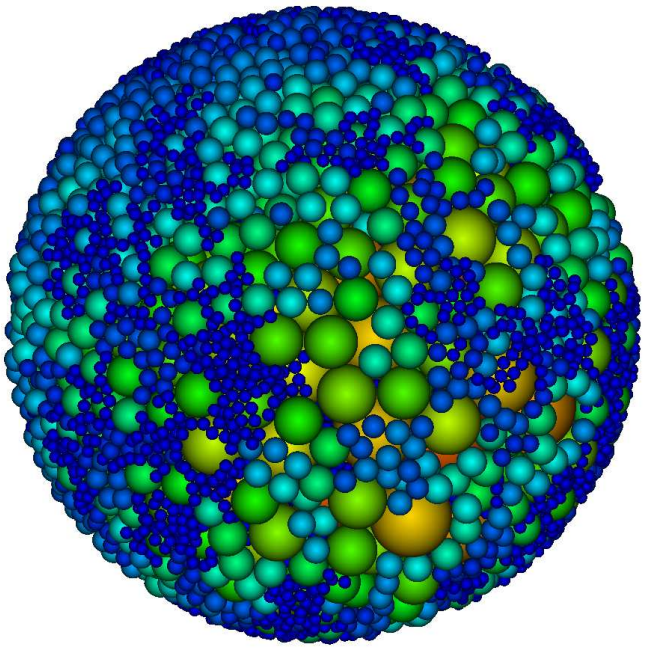

Fig. 7 Layer-wise arrangement in spherical boundary. Particles with similar sizes have priority to be placed next to each other.

2.3 Stabilization

The two typical options for achieving a firm and stable state of soil specimens are either the application of gravity for releasing unstable particles or the implementation of loads on the boundaries of the specimen. Both of these methods reduce the specimen volume by a small proportion. Therefore, when stabilization is required, the initial volume to be filled with particles to form the specimen should be a little larger to meet the desired porosity. The best results have been achieved with $3\% - 5\%$ larger final volumes. If the initial container is set too large, there might be some compaction difficulties later.

To achieve an exact predefined volume, that is, a desired porosity, one, two or three lids of the specimen container can be assigned a small, fixed velocity for a gradual compaction in one, two or three dimensions respectively.

The stabilization procedure for both application of gravity and active compaction is facilitated by DEM, which increases the specimen generation time. However, for the stabilization of the overall specimen only minor movements of the particles with a small velocity are required resulting in a relatively short computation time. The calculation time step, *dt*, might be longer and the list of surrounding particles can be updated less frequently [20]. As a result, the overall generation time using the new sequential method is still much shorter than using DEM only for generating particle packing. In this current study, the time step is input manually after several trials. However, to avoid unreal overlap between particles, it should satisfy the condition that:

$$dt \leq \frac{\delta_a}{2v_{max}} \tag{5}$$

Where: v_{max} - maximum velocity of particles; δ_a - acceptable overlap between particles.

Therefore, the more slowly the particles move, the faster the stabilization. When particles are stable, the load and/or the particle weight are supported by the normal contact forces. This normal contact force $\mathbf{F_n}$ in each contact is estimated by [21,22]:

$$\mathbf{F_n} = K_n \delta \mathbf{n} \tag{6}$$

Where: $\mathbf{F_n}$ - normal stiffness; δ - overlap distance; $\mathbf{n}$ - normal direction.

The tangential contact force, $\mathbf{F_t}$, during the collision is bounded by the Coulomb limit [11] and is estimated by:

$$\mathbf{F_t} = min(K_t \delta_t, \mu \mathbf{F_n})\mathbf{t} \tag{7}$$

Where: δ_t - tangential displacement [23]; μ - friction coefficient; and $\mathbf{t} = \mathbf{v_t}/v_t$ with $\mathbf{v_t}$ - tangential velocity. The viscous force, $\mathbf{F_v}$, is added to dissipate the energy and simulate the inelastic collisions [22]:

$$\mathbf{F_v} = G_n m_e v_n \mathbf{n} + G_t m_e v_t \mathbf{t} \tag{8}$$

Where: G_n, G_t - normal and tangential dissipation constants respectively, m_e - effective mass of the colliding particle pair, v_n normal velocity.

The environmental viscous force, $\mathbf{F_{vv}}$, acting on each particle is calculated, if needed, by the energy dissipation parameter, G_v:

$$\mathbf{F_{vv}} = -G_v m \mathbf{v} \tag{9}$$

Where: m - mass of particle, $\mathbf{v}$ - velocity.

To simulate the roughness of particles, Mechsys employed rolling stiffness, β, which is calculated from tangential stiffness [7]. This method avoids the rolling of spherical particles with high angular velocity at one position. The parameters of a simulation are represented in Table 1 as a sample.

If the stabilization focuses only on a simple static output, the tangential force and rolling velocity can be omitted to increase the calculation speed.

Table 1 DEM simulation parameters

Parameter	Value	Unit
Normal stiffness, K_n	2.00E+07	N/m
Tangential stiffness, K_t	2.00E+07	N/m
Normal viscous coefficient, G_n	1.60E+04	s^{-1}
Tangential viscous coefficient, G_t	1.60E+04	s^{-1}
Time step, dt	3.16E-08	s
Intermediate output time, d_{tout}	3.16E-03	s
Maximum total time of simulation, t_f	1.26E+03	s
Stop limit kinematic energy, K_s	1.07E+02	Nm
Rolling stiffness coefficient, β	0.12	N/m
Plastic moment coefficient, η	1	Nm

3 Results and discussion

3.1 Specimen generation time

The generation of a packing of individual particles using DEM simulation depends on many factors, such as the optimization of the code, the selection of time steps, the frequency of updating loops, and the energy dissipation ratio [24]. In the present study the DEM code of the Mechsys library was employed in order to compare the resulting calculation time with the performance of the new sequential packing method. The DEM code was used in a rather conventional way to create specimens in an instant procedure. The sample input parameters for the DEM model can be found in Table 1. The optimum verlet distance α is determined automatically by fitting equation [20] and the time step is adjusted by several steps, based on Equations 5 and [24].

The stabilization of specimens and instant packing process were run on 6 threads, while the sequential packing process was conducted by a single thread in a Macondo Cluster, which has 128 cores @ 2.20GHz. Even in this unfair condition, the new method produces a good performance. In the future, when there is a strong need for specimens with more than 10^6 particles, the checking steps (step 5, 10), which are the most time consuming steps, should be parallelized to reduce the calculating time. In the optimal case, this checking time is currently proportional to the triangular number, which is the sum of all integer numbers not larger than the number of particles. Hence, it has a complexity proportional to the square of the amount of particles. Since a fully optimized DEM has a linear complexity, it is expected that for a critical number of particles this performance trend will actually reverse with the DEM outperforming the sequential packing algorithm. However, this critical value seems to be considerably higher than the number of particles in samples considered here.

Although the result should depend on many factors, a survey on some typical packing processes showed that the new sequential packing method consumes much less time than DEM for the surveyed specimens (see Table 2) . In addition, most of the calculation time is spent on the stabilization, which adopts DEM.

It is evident from the table that narrow-graded soil specimens are generated faster by both methods. In terms of the sequential packing process, when a particle is not fit to a face, the face can be marked as closed immediately because all other particles have the same size. Regarding the instant packing, the maximum particle velocity, v_{max}, will reduce because there are no significantly smaller particles, which can move rapidly because of only one gentle collision. Therefore, the time step, dt, will increase because of Equation 5.

The statistics on some specimen generations (Figure 8) represents the range of calculating time to pack a maximum of 10^5 particles. It is obvious that the calculation time for uniform soils is marginal. However, this time soared with the increase in the number of particles and the number of intervals, ni, which is selected to ensure that the mean size of an size interval is not smaller than 0.9 of the mean size of the next larger interval. Besides, Figure 8 also shows a threshold by number of particles for some wide-graded PSD.

Against this background it is interesting to note that packing of uniformly sized particles can be quick if it employs simple, original DEM [21]. Moreover, when the rotation and friction of particles are neglected, the computation time by DEM reduces significantly. Also the type of specimens is acceptable if there is no serious requirement about contacts and overlaps between particles. A recent approach [25] could simulate behaviour of 10^5 dropped uniform particles in real time. However, the impressive calculation speed is achieved rather by using hardware efficiently than by an improvement in the packing algorithm [26].

Overall, the presented comparison shows that the new sequential packing method consumes much less time than DEM alone (Table 2) . In this connection it is important to bear in mind that most of the calculation time is spared on the stabilization, which adopts DEM.

The disadvantage of the sequential packing method is its inevitable long queue. Therefore, it is too early to say that the new method is better than instant methods. Nevertheless, it is evident that this method is fast and good for generated specimens with less than 10^5 particles. Furthermore, this method provides good control on particle position, porosity and size distribution.

Table 2 Packing time comparison*

Particle type	Number of particles	Sequential packing			Instant packing
		Packing time	Stabilizing time	Total time	
Uniform	1.0E+03	3.3E+00	9.1E+02	9.2E+02	4.3E+03
	1.0E+04	5.2E+01	1.1E+04	1.10E+04	6.5E+04
	1.0E+05	6.3E+02	2.5E+05	2.5E+05	4.1E+05
D_{max}/D_{min}=20	1.0E+03	**	1.5E+03	1.5E+03	9.9E+03
	1.0E+04	1.1E+02	1.5E+04	1.5E+04	1.4E+05
	1.0E+05	5.5E+04	3.6E+05	4.1E+05	> 6.0E+05

*Time unit is second (s); ** Not enough particles to get the size ratio

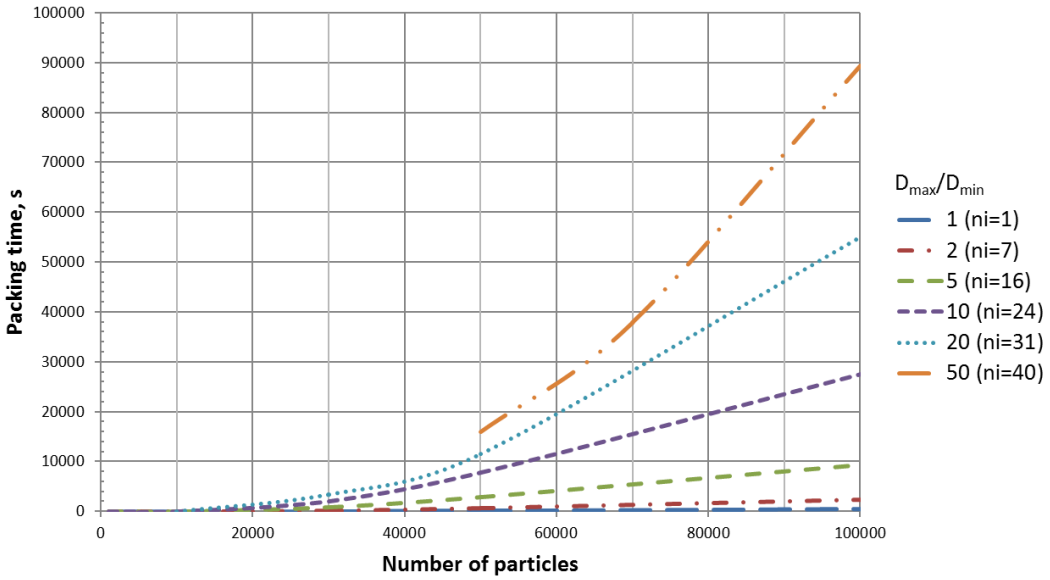

Fig. 8 Packing time by the new method. A pack of 100000 uniformed particles (blue line) can be generated after a minute, while a similar pack of wide-graded soils (orange line) can take more than one day, due to the particle selection and adjustment. An added particle might be selected from ni size intervals of the particle size distribution by priority or randomly.

3.2 Arrangement study

One important advantage of the new packing method is the possibility of varying the arrangement of particles by setting different rules of how particles are selected for building up new assemblies. This feature of the program is of vital importance for many characteristics and behaviours of soils, such as the internal stability of force chains and the hydraulic conductivity, which is directly influenced by the pore size distribution and thus the assembly of particles. In this paper two typical ways of arranging particle, layer-wise and discrete, are studied. These arrangements differentiate in terms of the local PSD (Figure 9).

The layer-wise arrangement of particles has a very practical meaning since it represents the arrangement of segregated soils when they are for instance dumped from trucks on construction sites [27]. The coarse particles will roll quickly down the dump heap simply because of its size. These particles forming an assembly of coarse particles. Meanwhile, fine particles, which are more influenced by friction and rolling resistance, are suspended and settle slower in the existing structure of a dump. As a consequence, it is more probable that particles with similar size will be located next to each other (Figure 9). The discrete arrangement, which allocates fine particles among coarser ones, is used as a benchmark because it is close to the random distribution of homogeneous soils (Figure 9).

One of the most conspicuous quantitative differences between these arrangements is the coordination number (Figure 10), which is estimated as the average number of contacts a particle has [28,29]. Statistics on generated specimens show a similarity in contact distribution with some prior studies on the coordination number of graded soils [5,30]. Those previous studies employed a lognormal PSD having a small amount of fine particles, which made most particles have more than four con-

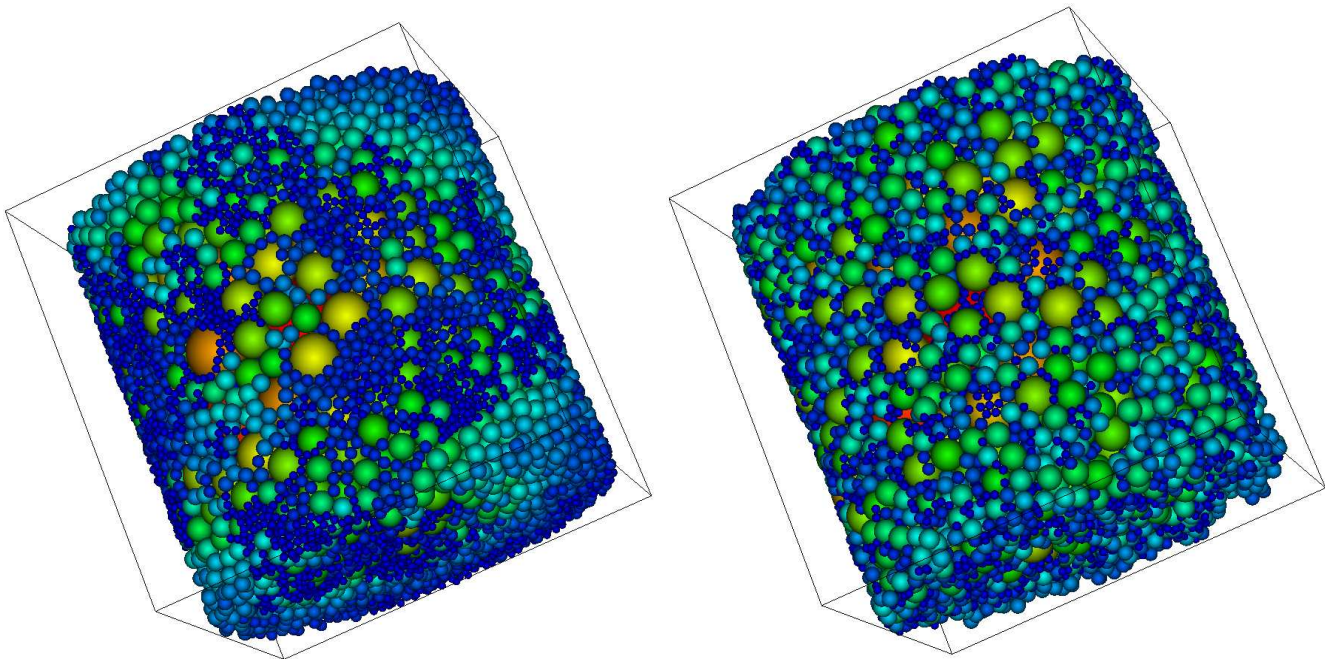

Fig. 9 Particle arrangements in cylindrical boundaries: layer-wise arrangement (left), where particles with similar sizes have priority to be placed next to each other; and discrete arrangement (right) - a random-wise arrangement, where small particles have priority to be placed between coarse particles.

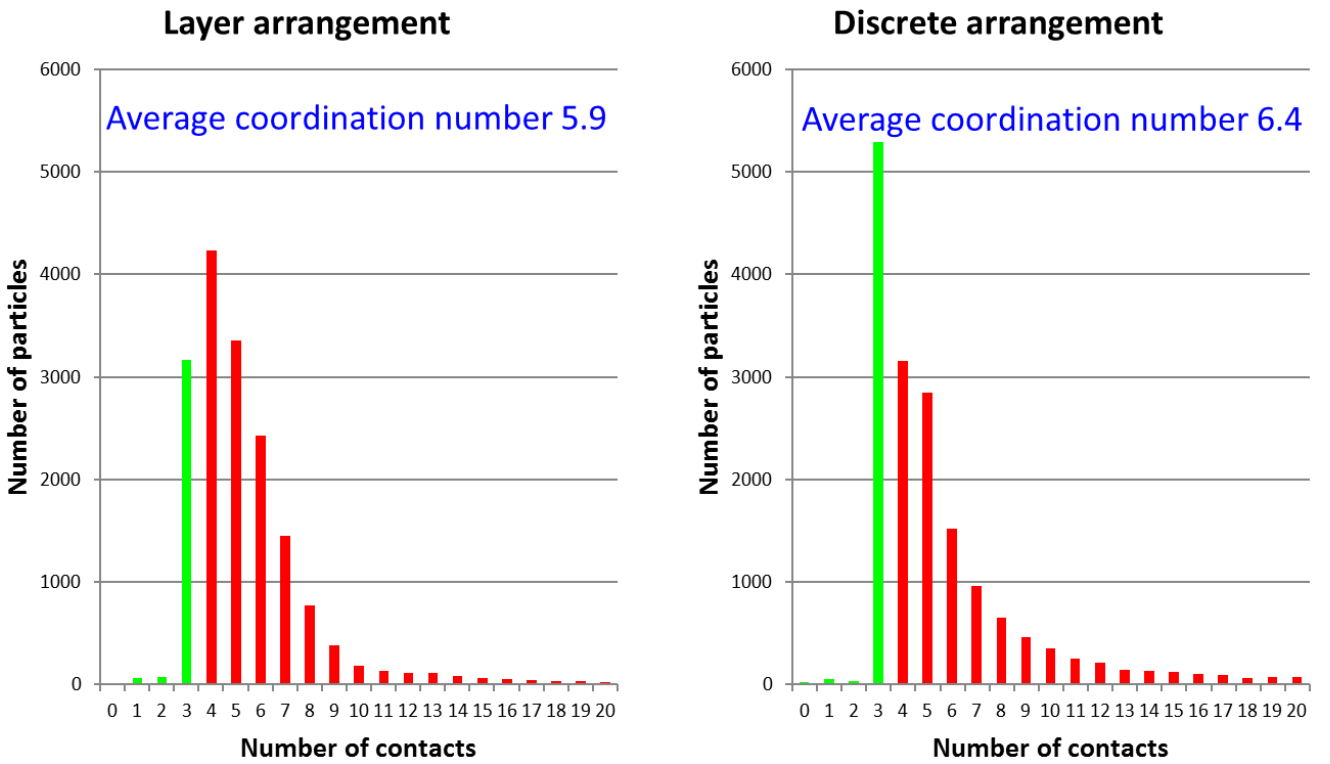

Fig. 10 Particle contacts in two different arrangements with the same particle size distribution D_{max}/D_{min} =20. Although their coordination numbers are similar, the discrete arrangement has more particles with less than 4 contacts, as well as particles with more than 8 contacts.

tacts. Nevertheless, there were surprisingly plenty of particles with less than three contacts in those studies.

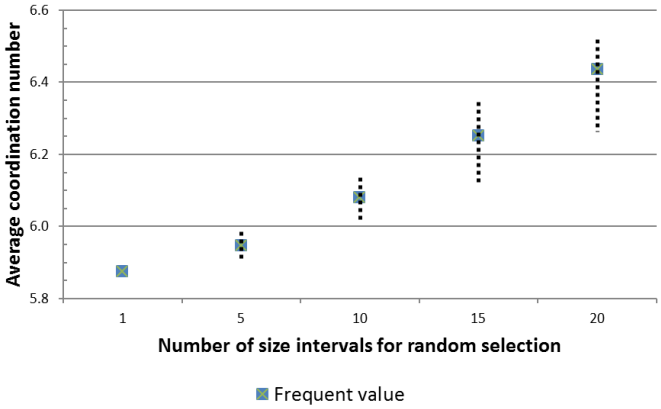

Fig. 11 Coordination number with random particle selection from different numbers of size intervals. A particle size distribution (D_{max}/D_{min}=20) is divided into 20 intervals. Particles are added by descending order. When an added particle do not fit to the face, it can be exchanged with another particle by random selection from a number of size intervals smaller than it.

The difference in the coordination number distribution of the two surveyed arrangements (Figure 10) is explained by their spatial distribution. In discrete arrangements, coarse particles have more contacts than themselves in layer-wise arrangements because smaller surrounding particles occupy smaller solid angles. Contrariwise, fine particles have fewer contacts because of their huge neighbours in the small surrounding space (Figure 10).

Note that the added particle in the layer-wise arrangement always is selected by descending order of particle size. Therefore, there is no randomness in packing. If the added particles are selected randomly from several large size intervals, the coordination number will increase with some random fluctuation. However, the arrangement will turn from a layer-wise to a discrete one. The statistics on several packs with different numbers of size intervals for particle selection are shown in Figure 11. The extreme values are not the theoretical limits, but empirical suggestions, which are approached after several packs. The most frequent values are marked as references. Theoretically, the coordination number should vary from the minimum value in layer-wise arrangements to the maximum value in discrete arrangements.

In terms of load transfer, stable and firm contacts capable of transferring mechanical load and thus stresses can be formed by larger particles only when they are in contact with each other (Figure 13). Already small deformations can move small particles out of the force chain. Thus, layer-wise arrangements with have a higher probability of larger particles neighbouring each other to create more force chains than discrete arrangements [31]. This observation becomes even more obvious when the size ratio D_{max}/D_{min} increases.

3.3 Approachable porosity range

The new sequential packing method without the subsequent compaction using DEM is basically a replacement for the dropping and rolling procedures normally conducted in DEM to prepare a specimen for a given PSD [6]. While in DEM the porosity is a random result from the procedures used to prepare the specimen, the new sequential packing method offers much better control over the resulting porosity. The two main steps in the procedure controlling the porosity are the selection of particles in the first loop (step 4) and the procedures used to fill voids of existing arrangements included in the second loop (steps 9 - 12).

Generally speaking, in the first loop of arranging particles, discrete arrangements result in larger porosities than layer-wise arrangements. The reason for this is simply the fact that in discrete arrangements larger particles tend to be located farther from each other. However, in layer-wise arrangements, voids formed by existing assemblies of particles can be filled by smaller particles in the second loop resulting in smaller porosities.

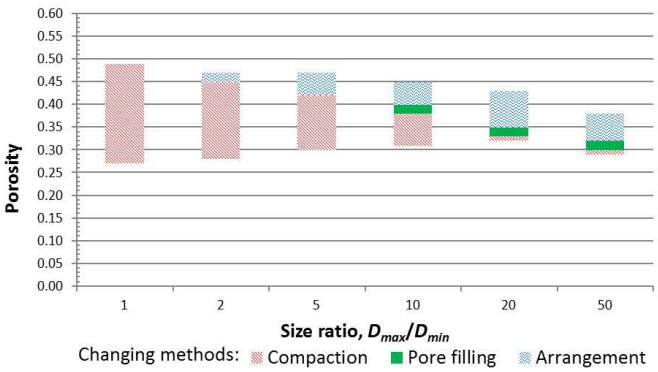

Fig. 12 Approachable porosity range by three different steps in the new sequential packing method: last compaction after packing (red), filling pore by the second loop (green), and packing order alternation in step 4 (blue).

The porosities which can be achieved with the new packing method are strongly dependent on the size ratio between the maximum and minimum diameter D_{max}/D_{min} of the PSD (Figure 12). Regarding narrow-graded soils, specimens are generated initially with high porosities. The reason for this is the inefficiency of the moving

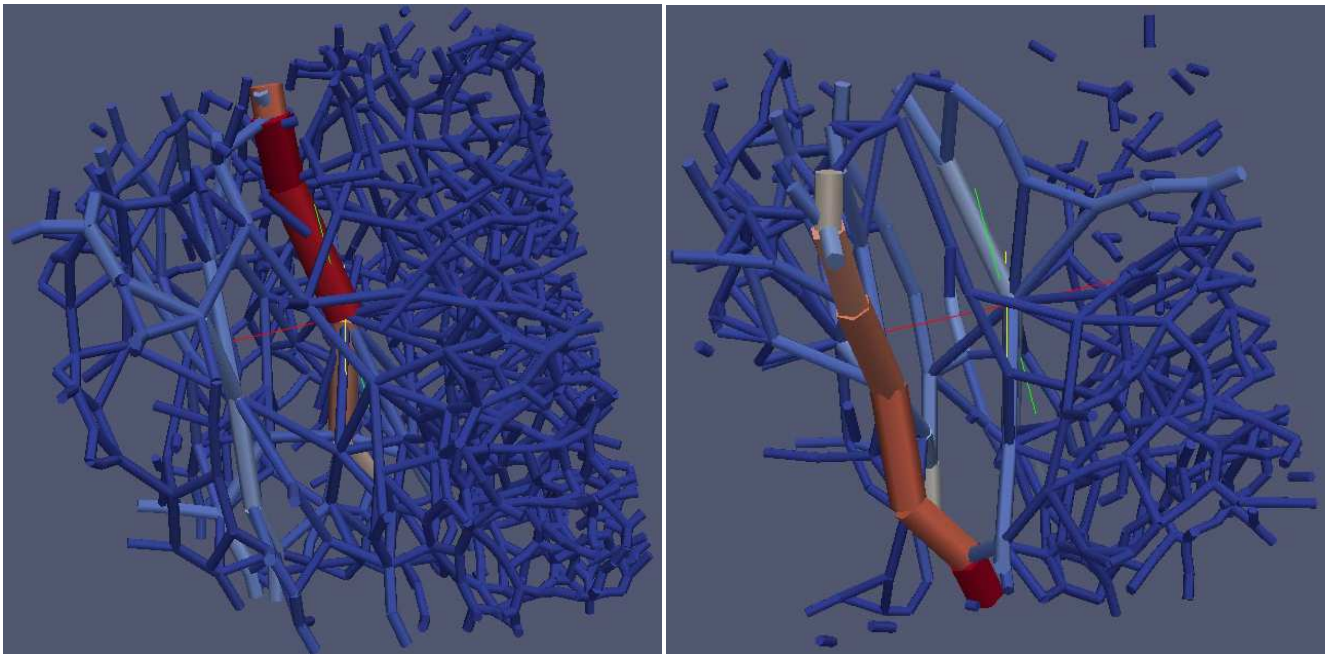

Fig. 13 Load distribution by force chains in: a) Layer-wise arrangement; b) Discrete arrangement (D_{max}/D_{min} =40)

and reselecting processes for particles with similar size. However, an efficient method in this case is to alter the porosity of the soil specimens by compaction using DEM, which is usually the last step for finalizing a specimen. For mono-disperse materials, compaction using DEM is the only method to achieve the desired porosity (Figure 15), which can vary between 0.27 and 0.49. The average coordination number for initial packing is approximately 6 [5], while this number in a dense specimen built mathematically is 12.

Due to the small pore sizes, the pore filling process by the second loop can be employed only when the size ratio is more than 5. However, the filling procedures are not very effective because of their shortcomings. For example, an added particle in the second loop is not moved to obtain a better position or reselected to fit in the pore. An improvement in the filling method is necessary to improve the variability of the porosity.

Contrariwise, subsequent compaction for large size ratios seems to be ineffective (Figure 16) because coarse particles tend to form one or several main force chains, which eventually prevent the sample from further compaction at some level(Figure 13).

Although the approachable porosity ranges are not huge, they already cover the majority of porosity ranges for coarse soils with spherical grains, which spreads from 0.26 to 0.49 [32].

3.4 Dealing with general shapes

Many practical problems dealing with more realistic behaviour of granular material require the representation of particles with non-spherical shapes. A very simple, but efficient approach for this problem is the consideration of non-spherical particles as circumscribed spheres (Figure 14). Subsequently, the packing algorithm is used exactly as presented, and as an additional step the circumscribed spheres are then substituted with their real particles. As a consequence of this approach, the resulting packing is generally very loose with high porosities. Furthermore, many particles are not touching each other and have various large distances between them, depending on the shapes of the non-spherical particles [33].

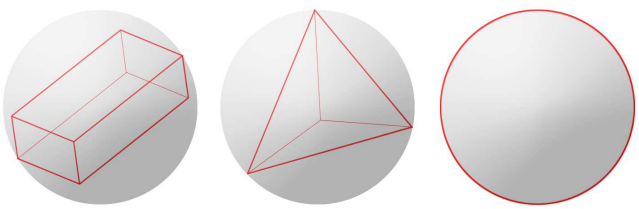

Fig. 14 Examples of non-spherical particles in their circumscribed spheres.

In order to create stable packing, a subsequent compaction step using DEM can be introduced. For this purpose, the bottom and top lids of the container are

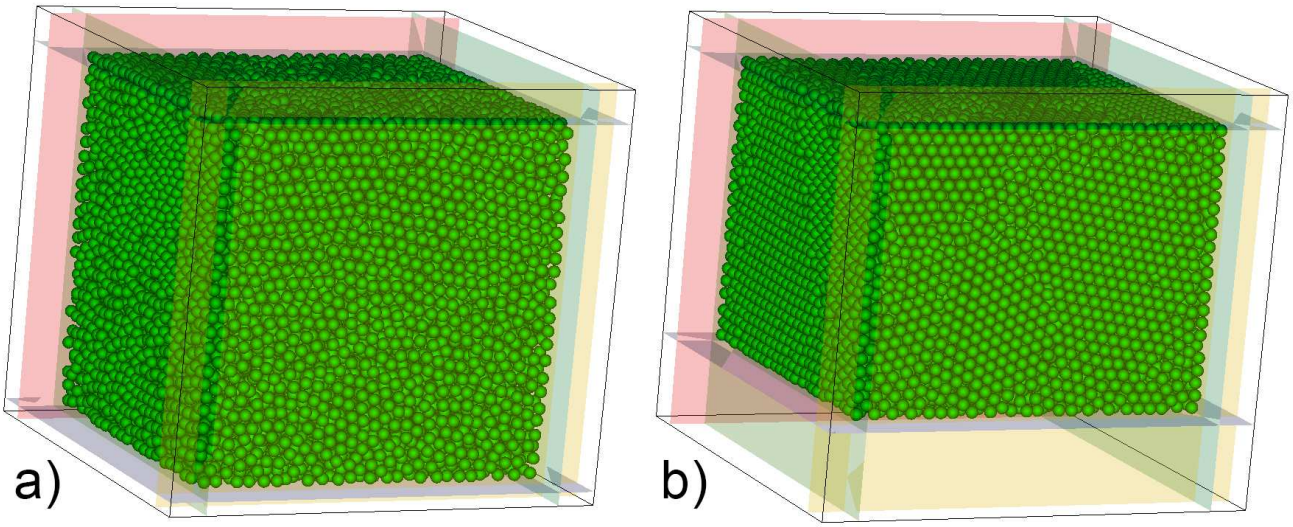

Fig. 15 Compaction of uniform particles as a last step for controlling the resulting porosity of a packing: a) before compaction; b) after compaction.

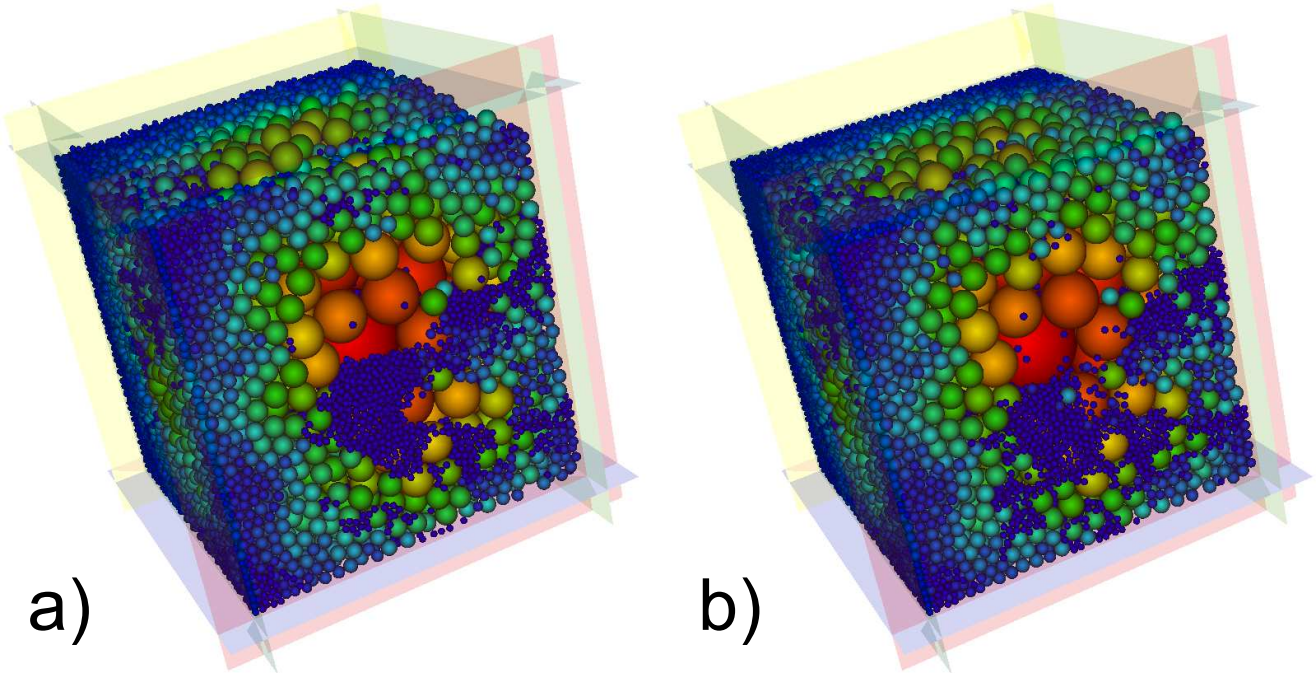

Fig. 16 Compaction of graded particles ($D_{max}/D_{min} = 20$): a) before compaction; b) after compaction. The particles resist well the compacting pressure.

assigned a small constant velocity toward each other until the desired porosity is reached (Figure 17). All particles are assigned a very high value of energy dissipation G_v . Therefore, they are attached to each other when the lids move. This method can provide segregated specimens in one dimension.

This approach is only a first step towards the representation of non-spherical particles within the new sequential packing method. A question to be solved, for example, is a step for controlling and varying the orientation of the non-spherical particles within the procedure.

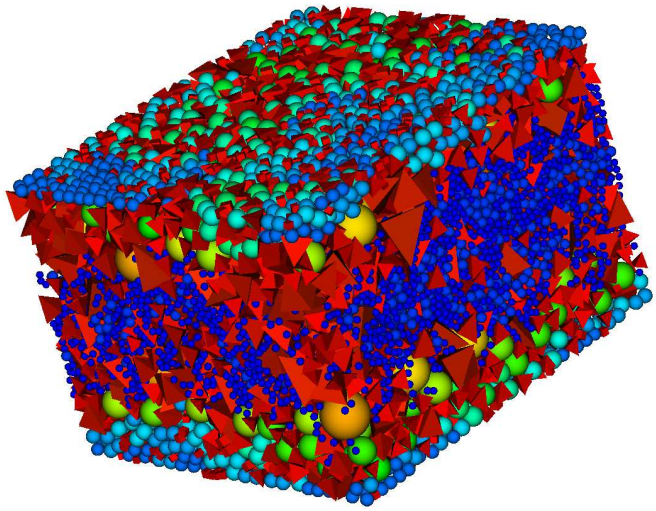

Fig. 17 Pack of particles with general shapes

4 Conclusion

This paper represents a novel sphere packing algorithm, which enables the controlled placement of particles sequentially into a predefined volume by solving analytically the trilateration equations. The new method allows the arrangement of particles with given PSD controlling the arrangement and porosity of the packing. Basically, the new method can be used even with very widely graded PSD. In the presented study, the largest size ratio between the largest and smallest diameter D_{max}/D_{min} is 50. The limitation for using this method with widely graded PSD is defined by the computational ability and memory of clusters.

The particle arrangement within the packing method is primarily controlled by the selection procedure of particles to be added to the existing arrangement. When particles with similar size have priority to be placed next to each other, the specimens tend to have layerwise arrangement. Otherwise, they seem to be more discrete and homogeneous.

The porosity is influenced also by the selection of new particles. Especially, when small particles are placed inside large voids of existing particle assemblies the porosity is further reduced with little change to the structural arrangement. The last step which further reduces porosity is compaction of the packing using DEM. In comparison to the actual packing of the particles, this compaction step can be far more computationally expensive. Overall, the required time for creating particle arrangements with the new method is smaller than conventional procedures using DEM.

The main advantage of the new packing method is the exact representation of the PSD, while two main characteristic of granular assemblies are controlled, namely structural arrangement and porosity. The latter could be varied in a range, which represents the real porosity of coarse-grained soils such as sands.

The current program does not use parallel calculation for the initial specimen generation. However, this is one important step of improvement to enable the processing of even wide PSDs which require the handling of much larger numbers of particles. Another improvement to be tackled in the future is the further development of the method to allow the use of non-spherically shaped particles.

The new method forms the basis for the investigation of important problems in geomechanics, such as filtration problems of granular structures and the anisotropy of hydraulic parameters. These problems require the realistic representation of basic characteristics of granular structures which can be now controlled using the presented method.

Acknowledgements The first author was granted a scholarship from the Vietnamese Ministry of Education and Training (MOET) and a top-up scholarship from the Discovery Project (DP120102188) Hydraulic erosion of granular structures: Experiments and computational simulations funded by the Australian Research Council. The simulations were based on Mechsys, an open source library and carried out using the Macondo Cluster from the School of Civil Engineering at The University of Queensland.

References

1. N. Reboul, E. Vincens, B. Cambou, Granular Matter **10**(6), 457 (2008)
2. T. Shire, C. OSullivan, Acta Geotechnica **8**(1), 81 (2013)
3. P. Winkler, M.S. Sadaghiani, H. Jentsch, K. Witt, in *Scour and Erosion: Proceedings of the 7th International Conference on Scour and Erosion, Perth, Australia, 2-4 December 2014* (CRC Press, 2014), p. 345
4. K. Bagi, Granular Matter **7**(1), 31 (2005)
5. A. Bezrukov, M. Bargieł, D. Stoyan, Particle & Particle Systems Characterization **19**(2), 111 (2002)
6. J. Rodriguez, C. Allibert, J. Chaix, Powder technology **47**(1), 25 (1986)
7. N. Belheine, J.P. Plassiard, F.V. Donzé, F. Darve, A. Seridi, Computers and Geotechnics **36**(1), 320 (2009)
8. J. Sherwood, Journal of Physics A: Mathematical and General **30**(24), L839 (1997)
9. S. Buechler, S. Johnson, International Journal for Numerical Methods in Engineering **94**(1), 1 (2013)
10. E. Oñate, S. Idelsohn, M. Celigueta, R. Rossi, J. Marti, J. Carbonell, P. Ryzhakov, B. Suárez, in *Particle-Based Methods* (Springer, 2011), pp. 1–49
11. S. Galindo-Torres, D. Pedroso, D. Williams, L. Li, Computer Physics Communications **183**(2), 266 (2012)
12. H.D. To, A. Scheuermann, S.A. Galindo-Torres, in *Infiltration instabilites in granular materials: theory and experiments* (2012)
13. H.D. To, S.A. Galindo-Torres. Dem gasket website (2014). URL `https://code.google.com/p/dem-gasket/`

14. Mechsys website (2014). URL `http://mechsys.nongnu.org/index.shtml`
15. B.T. Fang, Journal of Guidance, Control, and Dynamics **9**(6), 715 (1986)
16. H.D. To, A. Scheuermann, D.J. Williams, in *6th International Conference on Scour and Erosion (ICSE-6)* (Société Hydrotechnique de France (SHF), 2012), pp. 295–303
17. G. Langlet, Acta Crystallographica Section A: Crystal Physics, Diffraction, Theoretical and General Crystallography **35**(5), 836 (1979)
18. E. Sickafus, N. Mackie, Acta Crystallographica Section A: Crystal Physics, Diffraction, Theoretical and General Crystallography **30**(6), 850 (1974)
19. J.C. Lagarias, C.L. Mallows, A.R. Wilks, American Mathematical Monthly pp. 338–361 (2002)
20. S. Galindo-Torres, J. Muñoz, F. Alonso-Marroquin, physical review E **82**(5), 056713 (2010)
21. P.A. Cundall, O.D. Strack, Geotechnique **29**(1), 47 (1979)
22. S. Galindo-Torres, A. Scheuermann, H. Mühlhaus, D. Williams, Acta Geotechnica pp. 1–12 (2013)
23. S. Luding, Granular matter **10**(4), 235 (2008)
24. G.A. D'Addetta, *Discrete models for cohesive frictional materials* (2004)
25. S. Green, NVIDIA Whitepaper (2010)
26. J. Xu, H. Qi, X. Fang, L. Lu, W. Ge, X. Wang, M. Xu, F. Chen, X. He, J. Li, Particuology **9**(4), 446 (2011)
27. U. Saucke, J. Brauns, U. Schuler, Geotechnik Zeitschrift **22**, 259 (1999)
28. C.S. Chang, A. Misra, Journal of Engineering Mechanics **116**(5), 1077 (1990)
29. M. Oda, S. Nemat-Nasser, M. Mehrabadi, International Journal for Numerical and analytical methods in Geomechanics **6**(1), 77 (1982)
30. M. Powell, Powder technology **25**(1), 45 (1980)
31. H.D. To, S.A.G. Torres, A. Scheuermann, Acta Geotechnica pp. 1–13 (2014)
32. M. Budhu, *Soil Mechanics and Foundations, (With CD)* (John Wiley & Sons, 2011)
33. G.C. Cho, J. Dodds, J.C. Santamarina, Journal of Geotechnical and Geoenvironmental Engineering **132**(5), 591 (2006)